Proc. Natl. Acad. Sci. USA
Vol. 89, pp. 7222–7226, August 1992
Biochemistry

Dynamic NMR spectral analysis and protein folding: Identification of a highly populated folding intermediate of rat intestinal fatty acid-binding protein by ^{19}F NMR

(6-fluorotryptophan/protein stability/β-sheet)

IRA J. ROPSON AND CARL FRIEDEN

Department of Biochemistry and Molecular Biophysics, Washington University School of Medicine, St. Louis, MO 63110

Contributed by Carl Frieden, May 12, 1992

ABSTRACT **The folding of intestinal fatty-acid binding protein has been monitored by ^{19}F NMR after incorporation of 6-fluorotryptophan into the protein. The two resonances resulting from the two tryptophans of this protein showed different dependencies on denaturant concentration. One of the resonances was in slow chemical exchange between two resonance frequencies, native and completely unfolded. The changes for this resonance occurred over a denaturant concentration range identical to that monitored by circular dichroism or fluorescence during unfolding. The other resonance continued to show changes at concentrations of denaturant well above that needed to complete the unfolding transition as monitored by optical techniques. Site directed mutagenesis showed that tryptophan-82 was the residue responsible for the unexpected behavior. We conclude, based on complete lineshape analysis, that there are significant concentrations of one or more intermediates in equilibrium with the native and unfolded forms. The structure of the intermediate(s) is more similar to the completely unfolded form of the protein than to the native structure, since little if any secondary structure is present. Further, these structure(s) persist at high denaturant concentrations and may represent local initiating sites in the folding of this β-sheet protein.**

Proton nuclear magnetic resonance (^1H NMR) as a probe of protein structure is an extremely powerful technique, but the sheer number of signals generated by a protein frequently makes them difficult to resolve and assign. This is particularly a problem when a protein undergoes a large structural change, such as during folding and unfolding, since multiple signals will be present for each proton and the kinetics of exchange among the various states may affect the lineshape and position of the resonances. Although some progress has been made in the detection and characterization of transient intermediates by combining stopped-flow methods with NMR measurements of hydrogen–deuterium exchange (1–4), these methods detect the stabilization of hydrogen bonds during secondary structure formation and do not examine the conformation of side chains during the folding process. Information on the environment of side chains is particularly important because hydrophobic interaction among side chains is one of the driving forces responsible for protein folding (5). One means of simplifying the study of protein folding and probing side-chain interactions by NMR is the site-specific incorporation of a fluorine-containing amino acid residue.

Fluorine is a spin-½ nuclide that is present in 100% natural abundance and is similar in size to hydrogen. ^{19}F NMR is nearly as sensitive as ^1H NMR and the resonances occur over an extremely wide chemical shift range (6). Further, the chemical shift is extremely sensitive to changes in solvent environment, as would occur during the folding process. Since fluorine is not a naturally occurring atom in biological systems, the observed signals come only from the incorporated amino acids. Some caution must be exercised in the interpretation of ^{19}F NMR because the strength of the carbon–fluorine dipole or some other physical property of fluorine may significantly perturb structure and/or function. However, this seems not to be the case for a variety of systems examined thus far (6–10). In this paper we describe the use of ^{19}F NMR to study the folding at equilibrium of rat intestinal fatty acid-binding protein (IFABP) into which 6-fluorotryptophan (6FTrp) has been incorporated.

IFABP belongs to a family of small intracellular hydrophobic-ligand-binding proteins (11, 12). The crystal structure of holo-IFABP has been solved to a resolution of 2 Å (13) and that of apo-IFABP to 1.2 Å (14). The primary structural feature is two orthogonal β-sheets, of five strands each, enclosing a large cavity into which fatty acid binds. There are no cysteines or prolines in the primary sequence. The equilibrium and kinetic folding of this protein has been examined, primarily by monitoring fluorescence changes during the transition (15). Although no significant concentration of intermediates was detected at equilibrium by fluorescence, circular dichroism (CD), or absorption measurements, at least one transient intermediate was observed by kinetic measurements during either unfolding or refolding of this protein (15). Unfortunately, the earlier data could not determine which region(s) of the protein were responsible for the observed fluorescence changes. The current results on the equilibrium unfolding transition as monitored by ^{19}F NMR have begun to clarify the relationships among these structures.

MATERIALS AND METHODS

Mutagenesis. Mutagenic oligonucleotides were prepared to change each tryptophan codon to a tyrosine codon by site-directed mutagenesis using the uracil selection method of Kunkel *et al.* (16). Single-stranded phagemid DNA was produced in *Escherichia coli* BW313 from pMON-IFABP (17). Nucleotides, buffers, and enzymes for second-strand synthesis and ligation were from United States Biochemical. Mutants were identified and the entire coding regions were sequenced by the dideoxy method (18). Sequenase sequencing reagents and protocols were from United States Biochemical.

Protein Production. Large quantities of wild-type and mutant 6FTrp-containing IFABP were produced by the induction of protein synthesis in *E. coli* W3110trpA33, a tryp-

The publication costs of this article were defrayed in part by page charge payment. This article must therefore be hereby marked "*advertisement*" in accordance with 18 U.S.C. §1734 solely to indicate this fact.

Abbreviations: IFABP, intestinal fatty acid-binding protein; Gdn·HCl, guanidine hydrochloride; 6FTrp, 6-fluorotryptophan; T_2^*, effective transverse relaxation time; TFA, trifluoroacetic acid.

tophan auxotroph (19) provided by C. Yanofsky (Stanford University). Culture and induction conditions were similar to those used for the synthesis of 6FTrp substituted cellular retinol-binding protein II (7). Individual overnight cultures containing the various pMON-IFABP vectors were diluted 1:100 in M9 medium (20) supplemented with 1% Casamino acids, 1.5% glucose, vitamin B_1 (1 μg/ml), $FeCl_3$ (5 μg/ml), $ZnSO_4$ (0.4 μg/ml), $CuSO_4$ (0.8 μg/ml), $CoCl_2$ (0.7 μg/ml), $MnSO_4$ (0.5 μg/ml), H_3BO_3 (0.2 μg/ml), Na_2MoO_4 (0.7 μg/ml), ampicillin (50 μg/ml), and 0.1 mM tryptophan. Cultures were shaken at 37°C. After achieving an OD_{600} of 3.0, cells were harvested by low-speed centrifugation and resuspended in the same medium prewarmed to 37°C and containing 0.1 mM 6FTrp instead of tryptophan. The cultures were incubated at 37°C for 15 min and IFABP expression was induced by the addition of nalidixic acid (50 μg/ml). After 2 hr of induction at 37°C, the OD_{600} reached a value of about 5.5. Cells were harvested by low-speed centrifugation. Approximately 30 g of cells were produced from 5 liters of medium, resulting in 200–400 mg of purified protein after processing. The purification and delipidation protocols for mutant and wild-type [6FTrp]IFABP were identical to those reported for the unsubstituted wild-type protein (17). Incorporation levels were estimated by comparing the integrated intensity to that of a standard concentration of 2-fluorophenylalanine and were found to range from 80% to 90%. Purity was assessed by SDS/PAGE.

Ultrapure urea and guanidine hydrochloride (Gdn·HCl) were supplied by Schwarz/Mann. Solution preparation protocols, spectroscopic methods of monitoring protein unfolding at equilibrium, and data analysis have been described (15).

NMR Data Collection and Analysis. NMR data were collected on a Varian VXR-500 spectrometer operating at 470.268 MHz for ^{19}F, using a 5-mm Varian hydrogen/fluorine probe. The ^{19}F spin-lattice relaxation times were determined by the inversion recovery method and were <0.5 sec for all protein resonances. The pulse interval was 2.4 sec. Ninety-degree flip-angle pulses were calibrated for each sample and ranged from 7.8 to 19 μsec, at low and high ionic strength, respectively. An external chemical-shift and concentration standard, 2-fluorophenylalanine [−42.53 ppm from trifluoroacetic acid (TFA)], was used in a coaxial insert with all samples. No pH correction was made for 10–15% ^2H_2O content and no proton decoupling was used. Spectra were collected at 25°C and processed with 5 Hz of line broadening.

Spectral simulation and fitting were performed by the DNMR5 computer program (21) on a 25-MHz 80386 PC with math coprocessor (Gateway 2000, North Sioux City, IA). This program allows the variation of parameters in a system undergoing chemical exchange and optimizes the fit of a simulated spectrum to the actual data. The spectra at each concentration of denaturant in the transition zone were fit to two models, a simple two-state transition, $N \rightleftharpoons U$, and a three-state transition, $N \rightleftharpoons I \rightleftharpoons U$. The effective transverse relaxation time (T_2^*) for native protein and unfolded protein was calculated from the half-height linewidths (W) at 0 M and 4 M Gdn·HCl, respectively ($T_2^* = 1/\pi W$, where W is ≈40 Hz for the native resonances and 25 Hz for the unfolded resonances). The T_2^* of the intermediate was set equal to that of the unfolded protein, as discussed below. The following parameters were allowed to vary during the fitting procedure: the resonance frequency for each of the two 6FTrp resonances in each of the states, the relative population of each state, the exchange rates between states, and the baseline intensity and tilt values. The raw intensity values at each chemical shift frequency between −45.6 and −47.6 ppm (≈1 Hz per point) were converted to an ASCII data file and normalized to integer values ranging from 0 to 30,000, where 0 and 30,000 were the lowest and highest intensity values, respectively, in preparation for program input.

One problem with the use of this program was related to the limitations of the fitting algorithm. T_2^* could not be varied independently for each resonance in each state. If the resonance associated with Trp^6 was identical in frequency and linewidth for the intermediate and unfolded protein, as discussed below, and multiple intermediate forms of Trp^{82} were present, the T_2^* of the Trp^{82} resonance would be much less than that of Trp^6. This was particularly a problem at higher concentrations of denaturant, where little if any native protein was present, and it is probably responsible for the relatively poor fits at those concentrations (e.g., see Fig. 3*C*, 5.0 M urea). The inability to vary T_2^* independently may have caused very high correlation coefficients (>0.99) between the exchange rates during the fit at higher concentrations of denaturant, making the estimates of rates unreliable for those concentrations. However, the relative populations of each state were much less affected.

RESULTS AND DISCUSSION

Properties of [6FTrp]IFABP. The substitution of 6FTrp for tryptophan in IFABP appeared to have very little effect on the overall physical behavior of the protein. The CD spectrum of both folded and unfolded [6FTrp]IFABP was identical to that of unsubstituted protein (I.J.R., unpublished data), suggesting that no significant changes in secondary structure have occurred. [6FTrp]IFABP bound oleate in a normal fashion with a binding constant similar to that of unsubstituted protein (D. Cistola, personal communication). The equilibrium unfolding profiles as monitored by CD were very similar to those of unsubstituted protein as well (I.J.R., unpublished data). The stability of the protein extrapolated to the absence of denaturant was reduced ≈0.1 kcal/mol, within the error of the measurement. In contrast, the replacement of tryptophan by tyrosine reduced the stability of the protein in the presence of denaturant by ≈0.3 kcal/mol for the mutation at Trp^{82} and by ≈1.0 kcal/mol for the mutation at Trp^6. As such, the substitution of 6FTrp for both tryptophans in IFABP is a more conservative replacement than the single substitution of tyrosine for either tryptophan.

^{19}F NMR of [6FTrp]IFABP. The ^{19}F NMR spectra of wild-type [6FTrp]IFABP in the presence of various concentrations of urea are shown in Fig. 1. Two separate resonances of approximately equal intensity were observed for folded [6FTrp]IFABP (Fig. 1, 1.0 M urea). Surprisingly, two resonances of equal intensity were observed for unfolded protein (Fig. 1, 8.0 M urea). The different resonance frequencies in unfolded protein are probably due to local amino acid sequence effects (22). Multiple resonances have been found for unfolded 6FTrp-substituted cellular retinol-binding protein (7) and for unfolded 6FTrp-substituted dihydrofolate reductase (S. Hoeltzli, personal communication). The frequency differences in the unfolded state reflect the extraordinary sensitivity of ^{19}F to local environmental effects (6).

Unexpectedly, at 5.5 M urea (Fig. 1), where the equilibrium unfolding transition for [6FTrp]IFABP and unsubstituted IFABP was complete as measured by CD or fluorescence measurements (15), the spectrum was not identical to that of fully unfolded protein (>7 M urea, Fig. 1). One of the peaks was much smaller than expected and ≈30% of the total expected intensity was absent. Similar results were found when Gdn·HCl was used as the denaturant, where the transition as measured by CD or fluorescence was complete by about 1.8 M Gdn·HCl, but when measured by ^{19}F NMR was not complete until >2.5 M Gdn·HCl (I.J.R., unpublished data). However, the peak intensities in the transition zone were somewhat different with Gdn·HCl than with urea as denaturant, suggesting that although the same mechanisms

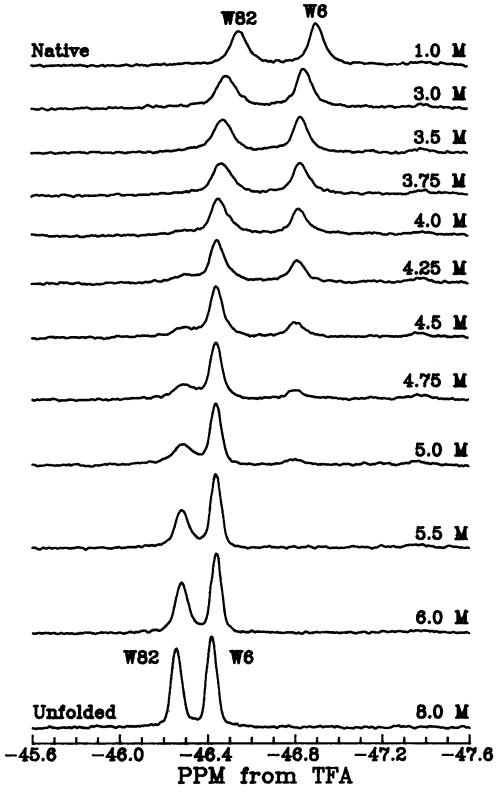

FIG. 1. ^{19}F NMR spectra of [6FTrp]IFABP at the concentrations of urea shown. Each spectra consisted of 512 transients. Solutions contained 20 mM phosphate, 0.1 M KCl, 0.1 mM EDTA, 10% ^2H_2O, and 0.7 mM [6FTrp]IFABP (11 mg/ml) and various concentrations of urea (1.0–8.0 M) and were adjusted to pH 7.2 at 25°C. Peaks due to 6FTrp residues at Trp^6 (W6) and Trp^{82} (W82) are indicated.

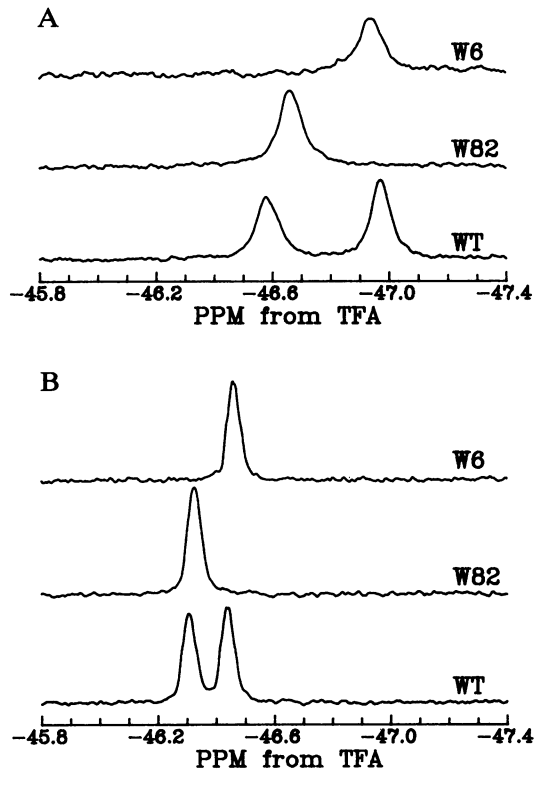

FIG. 2. ^{19}F NMR spectra of native (*A*) or unfolded (4.0 M Gdn·HCl) (*B*) [6FTrp]IFABP showing the resonance frequencies of the wild-type protein (WT), and the site-directed mutants containing only Trp^6 (W6) or Trp^{82} (W82). Each spectrum represents 512 transients.

were followed by the two denaturants, the rate constants and/or populations were different.

Since the two resonances behaved differently as a function of denaturant concentration, each tryptophan must see different environments during the transition from folded to unfolded species. Site-directed mutants converting each tryptophan to a tyrosine were made in order to assign the observed resonances in the folded and unfolded protein to an individual tryptophan. The resonance associated with Trp^{82} was found at higher chemical shift in both folded and unfolded protein (Fig. 2). Therefore, the Trp^{82} resonance was responsible for the unexpected missing intensity at 1.8 M Gdn·HCl and 5.5 M urea.

^{19}F NMR Spectral Simulation. The simplest and most likely explanation for the results presented in Fig. 1 is that some chemical exchange process among the various structured and unstructured states of the protein is occurring at a rate that causes line broadening and the loss of signal intensity. While several methods of determining rate constants and populations from these data can be used (23), the most precise and accurate method is the use of complete lineshape analysis to simulate and fit model parameters to the actual shape and intensity of the observed data (24).

Since the two resonances clearly behaved differently in response to denaturant concentration, it was unlikely that a simple model, $N \rightleftharpoons U$, would fit the data. It was found that a simple two-state model did describe the transition monitored by changes of the Trp^6 resonance but did not describe the missing intensity of the Trp^{82} resonance.

The fit to a sequential three-state model, $N \rightleftharpoons I \rightleftharpoons U$, was then examined. Initially, several different values for the T_2^* of the intermediate in the absence of exchange were tested, since the actual T_2^* of the intermediate could not be measured directly. The best fits were found when the T_2^* of the intermediate was set identical to that of the unfolded protein. The results of fitting this model at three concentrations of urea are shown in Fig. 3. An examination of the fit parameters at various concentrations of urea showed that the resonance associated with Trp^6 occurred at essentially identical frequencies (<5-Hz difference) in the intermediate and unfolded states of the protein, whereas the frequencies of the Trp^{82} resonance were significantly (>70 Hz) different from each other. This result implied that Trp^6 occupied only two environments, native and completely unfolded, whereas Trp^{82} inhabited at least three environments at equilibrium during the unfolding process, native, intermediate, and unfolded.

A plot of the concentration of the various states of the protein during an unfolding transition as predicted by the best fits to the three-state model is shown in Fig. 4. The significant intermediate concentration at equilibrium was unexpected, inasmuch as no intermediates had been detected by optical methods. The loss of the native intensity of Trp^6 was used to construct an equilibrium unfolding profile and was fit to a two-state transition (the line through the native data in Fig. 4). The parameters of the fit were virtually identical to those obtained previously by CD and fluorescence for unsubstituted IFABP (15), supporting the hypothesis that Trp^6 is found in only two environments, folded and unfolded.

Limitations of Modeling. There are some significant problems associated with the simulation and fitting of these models to the data. One crucial assumption was that the simplest model that fits the data was thought to be correct. It is probably an oversimplification to assume that Trp^{82} exists in only one intermediate conformation. For example, a transient intermediate was detected by stopped-flow fluorescence kinetics, although no significant concentration of this intermediate accumulated at equilibrium (15). Further, it is

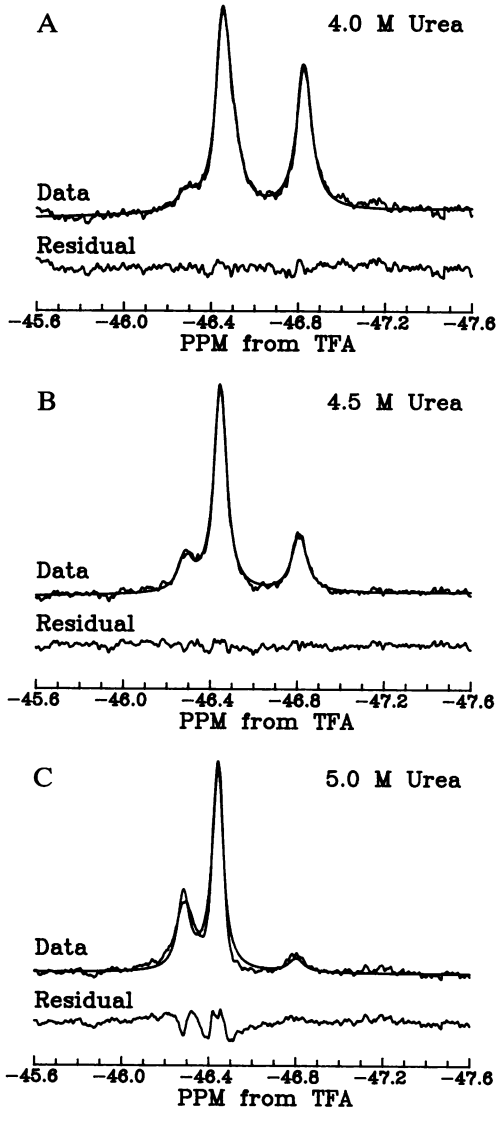

FIG. 3. ^{19}F NMR spectra of [6FTrp]IFABP in 4.0 M urea (*A*), 4.5 M urea (*B*), and 5.0 M urea (*C*). Each spectrum consists of 512 transients. The smooth line through the data was the best fit to a three-state model, $N \rightleftharpoons I \rightleftharpoons U$, with a single intermediate. The residual was the actual intensity minus the predicted intensity for the fit.

likely that several structures having similar chemical shifts could be exchanging rapidly with each other, but the data have insufficient resolution to differentiate among them. Although a three-state model fit the data, more complicated models connected by more complicated pathways would fit as well.

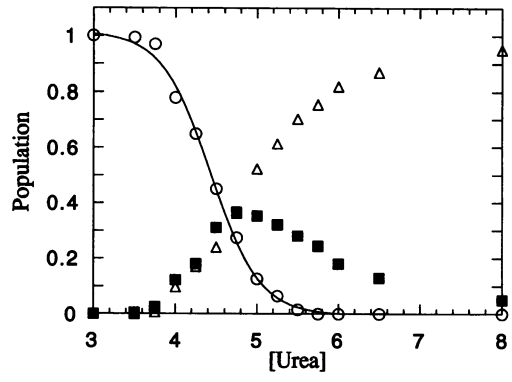

FIG. 4. Fractional population of each species in the transition zone as predicted by the fit to a three-state model, $N \rightleftharpoons I \rightleftharpoons U$. ○, Native; ■, intermediate; △, unfolded. The line through the native data was the fit of only the native population by nonlinear regression to a two-state transition, as described in the text.

Hypotheses on the Nature of the Intermediate. The data obtained here show that at least one intermediate is in equilibrium with the native and unfolded forms of the protein and that the intermediate involves the region of the protein in proximity to Trp^{82}. Furthermore, this intermediate persists at high denaturant concentrations. However, the actual nature of the interactions and the other residues that might be involved have not been identified. In the native structure, Trp^{82} is located in a hydrophobic pocket, surrounded by four phenylalanines and two leucines, with each aromatic amino acid on a different strand of the β-sheet (Fig. 5). Hydrophobic collapse has been implicated as the likely driving force in protein folding (5). This is the most hydrophobic region of the protein, and one could imagine a hydrophobic collapse during folding where these side chains are brought together rapidly, to reduce exposure to solvent without the formation of significant secondary structure. One might assume that during unfolding, these stabilizing interactions might be the last to break down. Hydrophobic interactions among aromatic groups have been found in unfolded bovine pancreatic trypsin inhibitor (25), unfolded lysozyme (26, 27), and unfolded α-lactalbumin (28). One implication of this model for initial events in the folding of IFABP was that a template for further folding was laid down by these tertiary interactions, forcing turns to occur at appropriate locations to maintain these contacts. This template effectively maps the locations and lengths of five of the β-strands of IFABP, serving as an initiating site for further folding. If this model for the folding of IFABP proves correct, the construction of a template of tertiary hydrophobic interactions prior to β-sheet structure formation would be an attractive general mechanism for the folding of antiparallel β-sheet proteins.

In another potential structure that could explain the observed results, the turn nearest Trp^{82} in the primary sequence of the protein (Glu^{85} to Lys^{88}) has the greatest stability. The

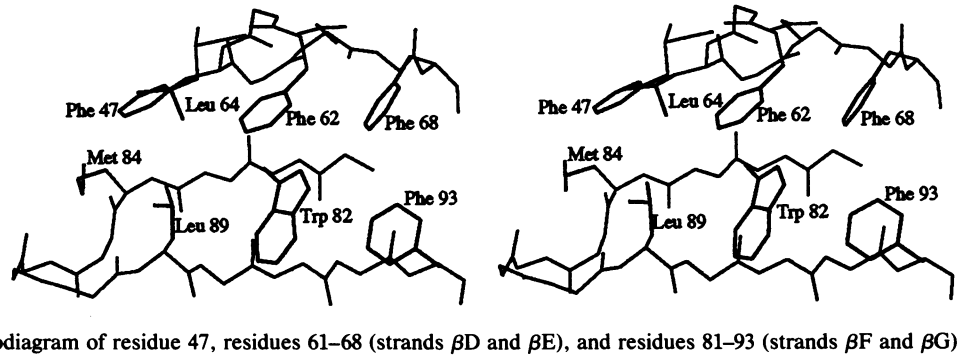

FIG. 5. Stereodiagram of residue 47, residues 61–68 (strands βD and βE), and residues 81–93 (strands βF and βG) of apo-IFABP.

observed chemical exchange phenomena would be caused by the rapid formation and dissolution of this turn at higher concentrations of denaturant. Since only a single reverse turn would be necessary, the CD signal of this structure would be very small and therefore would not be detected. It has been shown that isolated turns lacking proline can show structure in solution (29–31). There does not appear to be any obvious reason for stabilization of this turn relative to the other turns of this protein. However, hydrophobic interactions might stabilize turn structures. The formation of this turn would bring Trp^{82}, one of the phenylalanines, and one of the leucine discussed above into close proximity (Fig. 5). Alternatively, the turn between Glu^{63} and Asp^{67}, the closest turn to Trp^{82} in the three-dimensional structure of the native protein, could be the most stable turn. In this hypothesis, the anomalous behavior of the Trp^{82} resonance would be caused by a hydrophobic interaction between Trp^{82}, two phenylalanines, and a leucine that would be brought together by the formation of this turn (Fig. 5). Either of these structures would serve as an initiating site for protein folding, as shown by Monte Carlo simulations of β-protein folding (32). Further study is necessary to characterize the other residues that might be involved in these intermediates, in order to assess their importance in the folding of IFABP and to protein folding in general.

We acknowledge Dr. C. LeMaster for aid in using DNMR5, Dr. D. Cistola for general discussions on NMR methods, Dr. J. Sacchettini for the coordinates of the 1.2-Å-resolution structure of apo-IFABP prior to publication, and Dr. A. D'Avignon of the Washington University High Resolution NMR Service Facility, where the spectra were collected (funded in part by National Institutes of Health Biomedical Research Support Shared Instrument Grant 1 S10 RR02004 and a gift from the Monsanto Company). This work was supported by National Institutes of Health Grant DK13332 to C.F.

1. Bycroft, M., Matouschek, A., Kellis, J. T., Serrano, L. & Fersht, A. R. (1990) *Nature (London)* **346**, 488–490.
2. Miranker, A., Radford, S. E., Karplus, M. & Dobson, C. M. (1991) *Nature (London)* **349**, 633–636.
3. Roder, H., Elöve, G. A. & Englander, S. W. (1988) *Nature (London)* **335**, 700–704.
4. Udgaonkar, J. B. & Baldwin, R. L. (1988) *Nature (London)* **335**, 694–699.
5. Dill, K. A. (1989) *Biochemistry* **29**, 7133–7155.
6. Gerig, J. T. (1989) *Methods Enzymol.* **177**, 3–23.
7. Li, E., Qian, S., Nader, L., Yang, N. C., D'Avignon, A., Sacchettini, J. C. & Gordon, J. I. (1989) *J. Biol. Chem.* **264**, 17041–17048.
8. Luck, L. A. & Falke, J. J. (1991) *Biochemistry* **30**, 4248–4256.
9. Truong, H. T. N., Pratt, E. A., Rule, G. S., Hsue, P. Y. & Ho, C. (1991) *Biochemistry* **30**, 10722–10729.
10. Shen, Q., Simplaceau, V., Cottam, P. F., Wu, J. L., Hong, J. S. & Ho, C. (1989) *J. Mol. Biol.* **210**, 859–867.
11. Sweetser, D. A., Heuckeroth, R. O. & Gordon, J. I. (1987) *Annu. Rev. Nutr.* **7**, 337–359.
12. Gordon, J. I., Sacchettini, J. C., Ropson, I. J., Frieden, C., Li, E., Roth, K. A. & Cistola, D. P. (1991) *Curr. Opin. Lipidol.* **2**, 125–137.
13. Sacchettini, J. C., Gordon, J. I. & Banaszak, L. J. (1989) *J. Mol. Biol.* **208**, 327–339.
14. Scapin, G., Gordon, J. I. & Sacchettini, J. C. (1992) *J. Biol. Chem.* **267**, 4253–4269.
15. Ropson, I. J., Gordon, J. I. & Frieden, C. (1990) *Biochemistry* **29**, 9591–9599.
16. Kunkel, T. A., Roberts, J. D. & Zakour, R. A. (1987) *Methods Enzymol.* **154**, 367–382.
17. Sacchettini, J. C., Banaszak, L. J. & Gordon, J. I. (1990) *Mol. Cell. Biochem.* **98**, 81–93.
18. Sanger, F., Nicklen, S. & Coulson, A. R. (1977) *Proc. Natl. Acad. Sci. USA* **74**, 5463–5467.
19. Drapeau, G. R., Brammar, W. J. & Yanofsky, C. (1968) *J. Mol. Biol.* **35**, 357–367.
20. Sambrook, J., Fritsch, E. F. & Maniatis, T. (1989) *Molecular Cloning: A Laboratory Manual* (Cold Spring Harbor Lab., Cold Spring Harbor, NY), p. A.3.
21. LeMaster, C. B., LeMaster, C. L. & True, N. S. (1989) *Program QCMP059* (Quantum Chemistry Program Exchange, Indiana Univ., Bloomington).
22. Ropson, I. J., Gordon, J. I., Cistola, D. P. & Frieden, C. (1992) in *Techniques in Protein Chemistry III*, ed. Angeletti, R. (Academic, New York), pp. 437–443.
23. Sandstrom, J. (1982) *Dynamic NMR Spectroscopy* (Academic, New York).
24. Rao, B. D. N. (1989) *Methods Enzymol.* **176**, 279–311.
25. Roder, H. (1989) *Methods Enzymol.* **176**, 446–473.
26. Evans, P. A., Topping, K. D., Woolfson, D. N. & Dobson, C. M. (1991) *Protein Struct. Funct. Dyn.* **9**, 248–266.
27. Broadhurst, R. W., Dobson, C. M., Hore, P. J., Radford, S. E. & Rees, M. L. (1991) *Biochemistry* **30**, 404–412.
28. Baum, J., Dobson, C. M., Evans, P. A. & Hanley, C. (1989) *Biochemistry* **28**, 7–13.
29. Otter, A., Scott, P. G., Liu, X. & Kotovych, G. (1989) *J. Biomol. Struct. Dyn.* **7**, 455–476.
30. Sumner, S. C. J., Gallagher, K. S., Davis, D. G., Covell, D. G., Jernigan, R. L. & Ferretti, J. A. (1990) *J. Biomol. Struct. Dyn.* **8**, 687–707.
31. Liu, X., Scott, P. G., Otter, A. & Kotovych, G. (1990) *J. Biomol. Struct. Dyn.* **8**, 63–80.
32. Skolnick, J., Kolinski, A. & Yaris, R. (1988) *Proc. Natl. Acad. Sci. USA* **85**, 5057–5061.